BIREFRINGENCE OF TROPOMYOSIN CRYSTALS

TERESA RUIZ AND RUDOLF OLDENBOURG
Martin Fisher School of Physics, Brandeis University, Waltham, Massachusetts 02254

ABSTRACT   The birefringence of tropomyosin crystals was measured in the temperature range 5°–35°C. The experimental results are compared with a simple model calculation based on the theory developed by Wiener for the optical properties of colloidal systems. The difference between experimental and theoretical values is <15%, which denotes a good agreement given the simplicity of the model. A value of 0.011 was obtained for the intrinsic birefringence of the tropomyosin molecule. The temperature dependence of the crystal birefringence could be accounted for in part by a change of the unit cell parameters; this change was experimentally observed by others in x-ray diffraction experiments.

INTRODUCTION

Many proteins form clear, transparent crystals which show beautiful interference colors when viewed in a polarizing microscope. The interference colors arise from the anisotropy of the crystal refractive index, which in turn is due to the optical anisotropy of the protein molecules. The optical anisotropy of proteins or other macromolecules depends on their internal structure and on their overall shape. Therefore, the optical anisotropy or birefringence of macromolecules has attracted much interest as an experimentally accessible property which allows the study of molecular conformation. Most investigations have been done with macromolecular solutions with a partial alignment of the molecules induced by the application of an orienting agent such as a magnetic field (Maret et al., 1975; Maret and Dransfeld, 1985), an electric field (O'Konski and Haltner, 1957; O'Konski et al., 1959), or a shear force resulting from a velocity gradient in a flow experiment (Peterlin and Stuart, 1939; Lodge and Schrag, 1984). These experiments give valuable information on the solution properties of macromolecules, but the interpretation of the experimental results depends on the evaluation of both the optical properties of the molecules and their induced alignment. The alignment induced in macromolecular solutions is not measured directly; rather an orientation factor is derived from a theoretical model describing the alignment process. Accordingly, both the optical anisotropy and the orientation factor of the molecules are model–dependent and only a combination of both can be compared with experimental results. The structures of crystals, however, are usually known in great detail from x-ray diffraction and electron microscopy studies, and the optical anisotropy of a protein crystal can be related directly to the optical anisotropy of the protein molecules. Therefore, the birefringence of protein crystals is a touchstone for our understanding of the optical properties of macromolecules.

Measurements of the birefringence of protein crystals have been reported only twice: for hemoglobin crystals by Perutz (1953), and for lysozyme crystals by Cervelle et al. (1974). We describe a method of measuring the birefringence of protein crystals submerged in a solvent using a polarizing microscope with goniometer stage. We then report our experimental results for the birefringence of tropomyosin crystals. Tropomyosin is a 400 Å long α-helical coiled-coil protein that winds around the actin filaments of muscle. In the crystal, tropomyosin molecules link head-to-tail as they do in muscle, to form long filaments that run parallel to the body diagonals of the rectangular unit cell. The crystal contains ~96% solvent, and allows large-scale fluctuations of the filaments about their mean position. In fact, the crystal is a highly hydrated gel with a remarkable degree of order (Caspar et al., 1969; Phillips et al., 1986). We compare our experimental results of the optical anisotropy of tropomyosin crystals with the results of a simple model calculation. The calculation is based on the theory for the optical properties of colloidal systems first developed by O. Wiener in 1912. The theory treats a solute particle as a continuous dielectric imbedded in a continuous medium of different dielectric constant. Peterlin and Stuart (1939) take the same approach deriving the theory of birefringence induced in macromolecular solutions by an external field or by shear flow. Bragg and Pippard (1953) summarized Wiener's results and applied the theory to the birefringence of hemoglobin crystals measured by Perutz (1953) to derive the form anisotropy of the hemoglobin molecule. More recently, other theories for the optical anisotropy of macromolecules were developed in order to find agreement with birefringence data measured in flow experiments (Cassim and Taylor, 1965; Fortelny, 1974). The results of our model calculation for the birefringence of tropomyosin crystals are in very good agreement with the experimental data, supporting the applicability of Wiener's theory.

MATERIALS AND METHODS

Tropomyosin Crystals

The tropomyosin crystals were prepared from rabbit skeletal tropomyosin as described in Caspar et al., 1969, and were kindly provided by G.N. Phillips and C. Cohen. For our measurements, the crystals were immersed in their mother liquor (0.1 M sodium acetate, 0.05 M amonium sulfate, 0.001 M DTT, and 0.003 M NaN$_3$) and were kept inside thin walled sealed quartz capillaries (1 mm dia., 6 cm long). In order to minimize manipulation, the unusually fragile crystals were grown directly in the capillaries.

Polarizing Microscopy

For the polarizing microscope study, the capillaries were inserted in a specially developed goniometer stage. The goniometer was sitting in a temperature controlled water bath with glass windows. The water surrounding the capillary served as a heat exchanger to the capillary and as an index matching fluid to minimize the optical distortion caused by the cylindrical surface of the capillary. The goniometer allowed for 360° rotation angle around the long axis of the capillary and for a tilt angle of the capillary axis between 40° and 90° measured from the vertical. The water bath was sitting on the rotation stage of the polarized light microscope with a vertical light path. The crystals in the capillary were observed with the microscope using a low power objective lens (4×) with long working distance.

The propagation of light in anisotropic media, such as tropomyosin crystals, is usually an involved matter. However, our analysis is greatly simplified by two important observations: first, the birefringence of tropomyosin crystals is small ($\approx$0.001) and secondly, the crystals are immersed in a solvent matching very closely their average refractive index. Therefore, we have neglected the refraction of light at the solvent-crystal interface and the separation of the ordinary and the extraordinary light waves in the crystals. Under these assumptions, the birefringence Δn is the difference in refractive index for two mutually orthogonal polarized light waves traveling in the same direction through the crystal. For any given propagation direction, Δn is defined by the light waves which are polarized parallel to the two principal axes of the elliptical cross-section through the refractive index ellipsoid of the crystal. The cross-section through the ellipsoid is taken perpendicular to the propagation direction of the light waves. Because of the difference in refractive index, the two light waves undergo different retardations while propagating through the crystal. The difference in retardation or retardance R between the two waves is the product of the birefringence Δn with the optical path length d through the crystal:

$$R = \Delta n \times d. \tag{1}$$

R can also be expressed in terms of the wavelength λ_0 of the light in vacuum and the phase difference Φ between the two waves:

$$R = (\Phi \times \lambda_0)/2\pi. \tag{2}$$

When the two waves leave the crystal, their superposition produces a wave with elliptical polarization.

When illuminated with white light and viewed in the microscope between crossed polarizers, tropomyosin crystals showed beautiful patterns of interference colors. The different interference colors arise from the different optical path lengths through the wedge-like crystal. With the path length the retardance R varied across the sample cross-section. For values of R between a few hundred and a few thousand nanometers a particular interference color is associated with each value of R (see e.g., Hartshorne and Stuart, 1970). Hence, when the crystal was illuminated with white light, the varying optical path length was translated into a color pattern spread over the crystal cross-section.

The rotation stage of the microscope was used to find the extinction point for a given crystal orientation. When rotated to the extinction point,

all colors vanished and the crystal appeared black, merging with the dark viewing field of the microscope. In the extinction point the polarizer of the microscope is oriented parallel to one of the principal axes of the refractive index ellipse of the crystal. To measure the difference in refractive index between the two principal axes, the crystal was rotated out of the extinction point by 45° and a Berek compensator was inserted into the light path between the polarizer and the analyzer of the microscope. To compensate the retardance caused by the sample crystal, the fast axis of the compensator was oriented parallel to the slow axis of the crystal. Then, by means of a calibrated drum, the retardance of the compensator was set equal, but with opposite sign, to the retardance of the tropomyosin crystal. The compensation of the crystal retardance at a given point in the cross-section was determined by the disappearance of all interference colors at that point. The measured retardance is considered to be obtained at a wavelength of 550 nm which is the peak wavelength of the light used to illuminate the crystals. In one experiment we inserted interference filters in the optical path of the microscope to measure the birefringence at wavelengths 634, 515, 488, and 458 nm. The measured birefringence values were equal within the experimental error (5%).

For a given crystal orientation, we measured only the largest retardance, observed along the longest optical path through the crystal. To measure the longest optical path, the compensator was removed and the capillary was rotated around its axis by 90°. Then, with a second rotation around the horizontal axis of the goniometer, the capillary axis was rotated into the horizontal plane. The cross-section of the crystal now seen in the microscope exposed the full length of the largest optical path d through the crystal for which the retardance R was measured. After measuring d with a calibrated scale, the birefringence Δn was calculated from Eq. 1.

When the crystal was viewed down the crystallographic a-axis still another method was employed to measure the birefringence Δn_a. This method made use of the wedge formed by adjacent (101) faces with an interfacial angle of $\Omega = 44°$ (see Morphology). The path length for light propagating parallel to a increased linearly with the distance s from the edge of the wedge. The relationship between s, the wedge angle Ω, and the path length d is

$$d = 2s \times \tan (\Omega/2). \tag{3}$$

To determine Δn_a the retardance R was measured at several distances s from the edge of the wedge. The path length d was calculated with Eq. 3 for the given values of s. Then the retardance R was plotted against d and the slope of the linear fit through the data points was taken as the measured birefringence Δn_a for light propagating parallel to the crystallographic a-axis.

Averaged Optical Properties

The mean refractive index $\langle n \rangle$ of tropomyosin crystals can be derived from the refractive index increment $\partial n_{tr}/\partial c$ of tropomyosin solutions, and the concentration c of tropomyosin in the crystal:

$$\langle n \rangle = n_{solvent} + (\partial n_{tr}/\partial c) \times c. \tag{4}$$

The refractive index increment $\partial n_{tr}/\partial c = 0.187$ ml/g was measured at a wavelength of 436 nm and at 25°C by Holtzer et al. (1965). To extrapolate $\partial n_{tr}/\partial c$ to the wavelength of 550 nm and to 5° and 15°C, the temperature coefficient and the dispersion formula given by Perlmann and Longsworth (1948) were used. The concentration of tropomyosin in the crystal was calculated using the fact that four molecules are located in the unit cell:

$$c = 4 \times MW/N_A \times V_{uc} = 0.0513 \text{ g/ml},$$

with the Avogadro number N_A and the molecular weight MW = 68,000 Dalton for one tropomyosin molecule (Woods, 1967). The volume V_{uc} of the unit cell was calculated with the dimensions given in Fig. 4. The refractive index $n_{solvent}$ of the mother liquor in which the crystals were

suspended was calculated with a formula similar to (Eq. 4):

$$n_{solvent} = n_{water} + \Sigma \left[(\partial n_i/\partial c_i) \times c_i\right], \qquad (5)$$

with $\partial n_i/\partial c_i$ the refractive index increment and c_i the concentration of solute i. Only the 0.1 M sodium acetate and the 0.05 M amonium sulfate gave nonnegligible contributions. Their respective $\partial n_i/\partial c_i$ values and also n_{water} were taken from handbooks. Values of $n_{solvent}$ at different temperatures were derived by taking the appropriate values of n_{water} at those temperatures. All calculated values are summarized in Table I. The table also includes the averaged protein refractive index $\langle n_2 \rangle$ which was computed from (Eq. 4) by setting c equal to the inverse of the partial specific volume v of tropomyosin. Values of v were taken from Kay (1960) and extrapolated to the ionic strength of 0.2 M. v was also used to derive the volume fraction f of the tropomyosin molecules in the crystal:

$$f = V_{protein}/V_{unit\,cell} = c \times v.$$

RESULTS

Morphology

Tropomyosin forms a variety of ordered aggregates (Caspar et al., 1969). Our crystals were ~1 mm long and had the characteristic morphology first observed by Tsao (see Bailey, 1954). The crystals are orthorhombic (rectangular unit cell) dodecahedra bounded by {101}, {110}, and {011} faces. The indexing has been established by comparing the axial ratios calculated from interfacial angles measured optically with the unit cell dimensions known from x-ray patterns (Phillips et al., 1986). For example, the following interfacial angles were measured by us using the rotation stage of the microscope and viewing the crystals with the indicated orientation:

crystal viewed down the a-axis:

$$[\{011\}\wedge\{011\} = 80° \pm 2°,]$$

crystal viewed down the b-axis:

$$[\{101\}\wedge\{101\} = 45° \pm 2°.]$$

We observed usually large {011} faces with 5 sides and rectangular {110} faces. Faces within one family of faces were different in size. The crystals were elongated in the direction of the b-axis. A micrograph of a typical crystal is shown in Fig. 1 and a schematic drawing of the morphology can be seen in Fig. 2.

TABLE I

	5°C	15°C
$n_{solvent}$	1.3376	1.3370
$\langle n \rangle$	1.3469	1.3463
$\langle n_2 \rangle$	1.5899	1.5858
v [ml/g]	0.722	0.728
f	0.0370	0.0373

Compilation of calculated values of the solvent refractive index $n_{solvent}$, the average crystal refractive index $\langle n \rangle$, the average refractive index of tropomyosin $\langle n_2 \rangle$, its partial specific volume v and its volume fraction f in the crystal at temperatures indicated. Refractive index values are given for a wavelength of 550 nm.
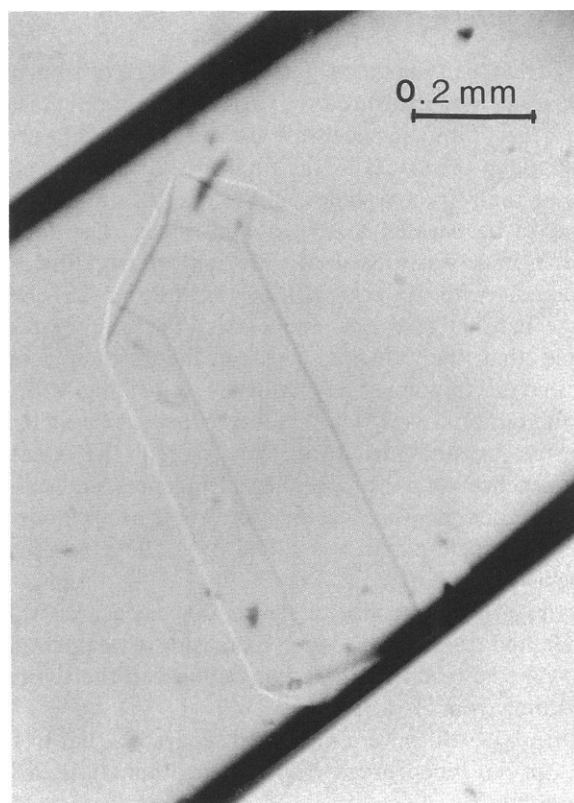

FIGURE 1 Tropomyosin crystal observed between two parallel polarizers. The crystal is oriented such that one of its two optic axes is parallel to the viewing direction. In this orientation the crystal appears to be optically isotropic. The crystal is immersed in its mother liquor and kept inside a sealed quarz capillary. The capillary is surrounded by water to minimize optical distortion by the cylindrical lens effect of the capillary. The dark diagonal lines at either end of the crystal are residual distortions from the capillary's walls.
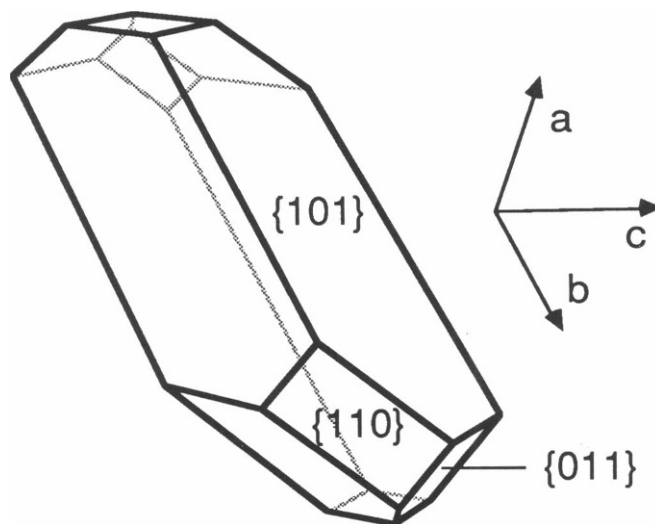

FIGURE 2 The morphology of the crystals used in this study is reproduced in this schematic drawing. Also shown are the crystallographic axes and the Miller indices of the planes associated with the crystal faces.

Birefringence

Measurements. The birefringence of tropomyosin crystals was measured for various crystal orientations. The largest birefringence was observed, when light propagated along the crystallographic b-axis, and the principal axes of the refractive index ellipse for this geometry was found to be parallel to the a- and c-axis. The smallest birefringence was measured with light propagating along the a-axis, with the principal axes of the refractive index ellipse parallel to the b- and c-axis. Therefore, we concluded that the principal axes of the refractive index ellipsoid of tropomyosin crystals is coinciding with the crystallographic axes. This result is expected for an orthorhombic crystal structure. We called the smallest birefringence Δn_a, the largest birefringence Δn_b, and the birefringence measured with light propagating along the crystallographic c-axis was called Δn_c. The experimental values are presented in Fig. 3. Fig. 3 also shows the temperature dependence of $\Delta n_{a,b,c}$. The measured values for Δn_a and Δn_b decreased with increasing crystal temperature, Δn_c, however, remained unchanged in the temperature range from 5° to 35°C.

All $\Delta n_{a,b,c}$ values were measured separately, but in fact, they are not independent from one another. It is easy to show that:

$$\Delta n_a = \Delta n_b - \Delta n_c.$$

All the measured values satisfy this relationship within the experimental error of 5%.

None of the three birefringence values $\Delta n_{a,b,c}$ are alike. This result indicates that tropomyosin crystals have a refractive index ellipsoid with three different principal axes. Such crystals have two optic axes, i.e., they are biaxial. The cross section perpendicular to an optic axis through the refractive index ellipsoid is circular. When light propagated parallel to an optic axis through a crystal,
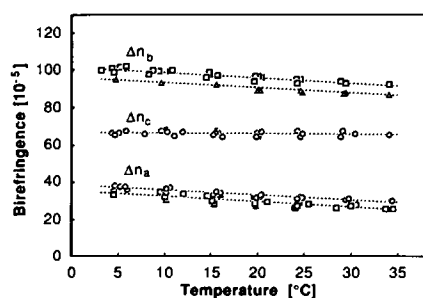
the crystal appeared to be optically isotropic. We observed that the optic axes in tropomyosin crystals are located in the a-c plane and the angle χ between the crystallographic a-axis and an optic axis was 37° ± 3° ($T = 5$°C). This measured value compares well with the value calculated with $\Delta n_{b,c}$ using a formula derived from geometric considerations for weakly birefringent crystals ($\Delta n_{a,b,c} \ll 1$):

$$\cos^2 \chi \approx \Delta n_c / \Delta n_b, \qquad \chi = 35°.$$

A micrograph of a crystal viewed down an optic axis is shown in Fig. 1

Model Calculation Our calculation of the optical properties of tropomyosin crystals is based on a simple rod model for the contents of the unit cell (see Fig. 1). In the crystal, the rods representing the tropomyosin molecules are connected and form straight, thin filaments. Four sets of parallel filaments can be distinguished in the crystal, each set has the same orientation as one of the four body diagonals of the rectangular unit cell. Contacts between filaments belonging to a different set are limited to small regions at each vertex and at the center of the unit cells. The filaments are mostly surrounded by solvent which occupies more than 96% of the crystal volume.

For the calculation of the refractive index of the crystal, the solvent was assumed to be a transparent, isotropic medium with the refractive index n_1. The tropomyosin filaments were treated as infinite long, transparent rods with a refractive index $n_{2\parallel}$ for light polarized parallel to the filament axis and $n_{2\perp}$ for light polarized perpendicular to the axis. The difference $\Delta n_2 = n_{2\parallel} - n_{2\perp}$ is called the intrinsic birefringence of the filament material. In the following calculations the dielectric constants ϵ_1, $\epsilon_{2\parallel}$ and $\epsilon_{2\perp}$ were used instead of the corresponding refractive indices, with the general relationship $\epsilon = n^2$.

The tensor $\underline{\epsilon}$ of the dielectric constant of the crystal can be written as (MKSA-system):

$$\underline{\epsilon} = \epsilon_1 + 4\pi\underline{\alpha}, \tag{6}$$

The main contribution to $\underline{\epsilon}$ comes from the solvent with an added polarizability $\underline{\alpha}$ equal to the sum of the excess polarizabilities of all the filaments. In (Eq. 6) and throughout this paper, polarizabilities are given per unit volume and are therefore dimensionless. The computation of $\underline{\alpha}$ is the subject of the remaining part of this section.

Let us consider an array of like particles with dielectric constant ϵ_2 embedded in a solvent with ϵ_1. The particles occupy a fraction f of the total volume V_T which is polarized by an external electric field. It can be shown (Bragg and Pippard, 1953) that the addition of one more particle to the array alters the dielectric constant ϵ in the same way as ϵ is changed by the addition of an induced dipole with the polarizability α_2:

$$\alpha_2 = \frac{V_c}{4\pi V_T} \frac{(\epsilon_2 - \epsilon_1)}{1 + (1 - f)\{(\epsilon_2 - \epsilon_1)/\epsilon_1\} L} \tag{7}$$

V_c is the volume of the particle added. The factor $(1 - f)$ in the denominator accounts for the fact that the presence of the other particles increases the field polarizing the particle just added (Lorentz correction). The depolarization factor L depends on the shape of the particle and on the mutual orientation between the electric field, polarizing the array, and the particle axis. For an infinite long rod such as a tropomyosin filament in the crystal, L is equal to zero, if the electric field is parallel to the rod or filament axis, and L is equal to $\frac{1}{2}$, if the field is perpendicular to the axis. Therefore, depending on whether the added filament is oriented parallel or perpendicular to the field, the corresponding dipole has the polarizability:

$$\alpha_{2\parallel} = \frac{V_c}{4\pi V_T}(\epsilon_{2\parallel} - \epsilon_1) \qquad (7a)$$

$$\alpha_{2\perp} = \frac{V_c}{4\pi V_T} \frac{2(\epsilon_{2\perp} - \epsilon_1)}{2 + (1 - f)\{(\epsilon_{2\perp} - \epsilon_1)/\epsilon_1\}} \qquad (7b)$$

By using $\epsilon_{2\parallel}$ and $\epsilon_{2\perp}$ rather than ϵ_2, we accounted for the possibility that the dielectric constant of the filament material might be anisotropic. The anisotropy of the polarizability of the added filament in the array of the other filaments is defined as:

$$\Delta\alpha_2 = \alpha_{2\parallel} - \alpha_{2\perp}. \qquad (8)$$

If the array of filaments is very dense, i.e., f is very close to 1, $\Delta\alpha_2$ reduces to $(\epsilon_{2\parallel} - \epsilon_{2\perp})V_c/4\pi V_T$ which is only nonzero if the filament material is anisotropic. However, if f is <1, $\Delta\alpha_2$ is nonzero even if the filament material is isotropic. In fact, $\Delta\alpha_2$ increases with increasing values for $(\epsilon_2 - \epsilon_1)$, i.e., the more different the dielectric constants are of the solvent and the filament material. This additional anisotropy of the polarizability is called form anisotropy.

In general, a filament is not oriented either parallel or perpendicular to an applied field, but has some oblique angle with the field. In this case, the induced dipole moment of the filament in an external field has to be figured from the polarizability tensor $\underline{\alpha}_2$.

In tropomyosin crystals there are four sets of filaments, each set is parallel to one of the four body diagonals of the unit cell. Therefore, the polarizability tensor $\underline{\alpha}$ from Eq. 6 can be written as the sum of four terms, each term stands for one set of filaments:

$$\underline{\alpha} = \underline{\alpha}_{[1,1,1]} + \underline{\alpha}_{[-1,1,1]} + \underline{\alpha}_{[1,-1,1]} + \underline{\alpha}_{[1,1,-1]} \qquad (9)$$

The indices indicate the crystallograhic direction associated with the corresponding set of filaments. The expressions for the different terms in (Eq. 9) are derived in the appendix.

The orthorhombic structure of tropomyosin crystals implies that $\underline{\alpha}$ attains a diagonal form, if it is expressed in the coordinates of the crystallographic axes. In other words, the principal axes of the polarizability tensor $\underline{\alpha}$ coincide with the crystallographic axes. The three terms of the diagonal form of $\underline{\alpha}$ are given in the appendix. When the

results are inserted into (Eq. 6), the following dielectric constants of the crystal for fields parallel to the crystallographic **a**-, **b**-, and **c**-axis are obtained:

$$\epsilon_a = \epsilon_1 + 4\pi[(a^2/l^2)(\alpha_{2\parallel} - \alpha_{2\perp}) + \alpha_{2\perp}] \qquad (10a)$$

$$\epsilon_b = \epsilon_1 + 4\pi[(b^2/l^2)(\alpha_{2\parallel} - \alpha_{2\perp}) + \alpha_{2\perp}] \qquad (10b)$$

$$\epsilon_c = \epsilon_1 + 4\pi[(c^2/l^2)(\alpha_{2\parallel} - \alpha_{2\perp}) + \alpha_{2\perp}] \qquad (10c)$$

a, b, c are the dimensions of the unit cell, l is the length of its body diagonal, and f is the volume fraction of the tropomyosin molecules in the crystal. The square roots of Eqs. 10, a–c are the crystal refractive indices for light polarized parallel to the crystallographic axes.

The values of all parameters in Eqs. 10, a–c and 7 a and b are known from experiment except for the intrinsic anisotropy of the dielectric constant of tropomyosin. However, the average refractive index $\langle n_2 \rangle$ of tropomyosin can be estimated from the refractive index increment $\partial n_{tr}/\partial c$ (see Materials and Methods and Table I). Therefore, we first assumed that the protein material has an isotropic refractive index and we set:

$$\epsilon_{2\parallel} = \epsilon_{2\perp} = \langle n_2 \rangle^2 = 2.5278 \qquad (T = 5°C). \qquad (11)$$

The crystal refractive indices can then be calculated directly from (Eqs. 10, a–c) without any adjustable parameter, with the following results:

$$n_a = 1.34624$$

$$n_b = 1.34670$$

$$n_c = 1.34702$$

From these values the birefringences for light traversing the crystal parallel to the crystallographic axes can be deduced:

$$\Delta n_a = n_c - n_b = 33 \times 10^{-5} \qquad (12a)$$

$$\Delta n_b = n_c - n_a = 78 \times 10^{-5} \qquad (12b)$$

$$\Delta n_c = n_b - n_a = 45 \times 10^{-5} \qquad (12c)$$

The calculated values for Δn_a, Δn_b, and Δn_c are remarkably close to the measured values shown in Fig. 3.

The values for $\Delta n_{a,b,c}$ calculated so far are systematically smaller than the measured ones. The assumption of a positive intrinsic birefringence Δn_2 in the tropomyosin filament brought the calculated values even closer to the measured ones. To account for the intrinsic birefringence, we set:

$$\Delta n_2 = n_{2\parallel} - n_{2\perp},$$

with

$$(n_{2\parallel} + 2 \times n_{2\perp})/3 = \langle n_2 \rangle.$$

To find the best fit to our experimental data, Δn_2 was varied, but $\langle n_2 \rangle$ was kept constant at the value given by Eq.

11. The best fit was obtained for $\Delta n_2 = 0.011$, with an agreement between experimental and calculated values now better than 15%.

We have observed a decrease in the measured birefringence Δn_a and Δn_b with increasing temperature; Δn_c, however, remained constant (see Fig. 3). For a possible explanation of this phenomenon we turned to an observation by Phillips (personal communication) who measured in x-ray diffraction experiments with tropomyosin crystals a slight change of the unit cell parameters, when the temperature was changed between 5° and 15°C. He observed (50% error margin):

$$a(15°C) = a(5°C) + 0.5\%, \quad (13a)$$

$$b(15°C) = b(5°C) + 0.1\%, \quad (13b)$$

$$c(15°C) = c(5°C) - 0.4\%. \quad (13c)$$

A change in unit cell parameters alters the dielectric constants computed from (Eqs. 10, a–c), and correspondingly the calculated birefringence values. Therefore, we entered the above values for a, b, and c at 15°C into (Eqs. 10, a–c), we changed ϵ_1 and ϵ_2 to their values at 15°C listed in Table I and then computed Δn_a, Δn_b, and Δn_c. Comparing the values calculated for 15°C with those calculated for 5°C showed that Δn_a and Δn_b decreased by $\sim 0.18 \times 10^{-5}$ per degree Celsius, whereas Δn_c decreased only by 0.07×10^{-5} per degree. This calculated temperature factor for Δn_a and Δn_b is somewhat smaller than the measured temperature factor given in the caption of Fig. 3. Interestingly enough, when we increased the percentage change of the unit cell parameters given in (Eqs. 13, a–c) by a factor of 2.5, the calculated temperature coefficients for Δn_a, Δn_b, and Δn_c got very close to the measured values, i.e., $\partial \Delta n_a/\partial T$ and $\partial \Delta n_b/\partial T$ increased to $0.29 \times 10^{-5}/K$, whereas $\partial \Delta n_c/\partial T$ decreased to $0.06 \times 10^{-5}\ 1/K$.

DISCUSSION

Birefringence

Our experimental results show some systematic variation in the birefringence values measured with different crystals (see Fig. 3). These variations are probably associated with variations in the unit cell parameters. Variations of up to 2% in unit cell parameters are observed in x-ray diffraction experiments with different tropomyosin crystals (Phillips, 1987; Caspar et al., 1969). Our model calculation has shown that the crystal birefringence depends sensitively on the unit cell parameters or, correspondingly, on the orientation of the rods.

The unit cell used in our model calculation (see Fig. 4) contains four straight rods representing the tropomyosin molecules. The four rods intersect with one another in the center of the unit cell. A more accurate model displaces the connecting point from the center of the unit cell along the c-axis by ~ 40 Å giving rise to a long and a short arm in
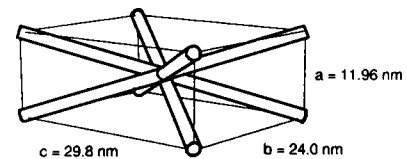

FIGURE 4 The unit cell used for our model calculation contains four dielectric rods extending along the four body diagonals of the rectangular cell. The rods represent the tropomyosin molecules which account for 3.6% of the volume of the unit cell. The remaining 96.4% of the cell volume are filled with solvent. The dimensions of the unit cell along the three crystallographic axes are also shown. For a more detailed model of the contents of the unit cell see Phillips et al. (1986).

each tropomyosin molecule with a slightly different orientation for each arm (Caspar et al., 1969). We modified our calculation to take this more accurate model of the unit cell into account, but the new results were not significantly different from the results obtained from the straight rod model.

Our calculations used the theory of continuous dielectrics to derive the birefringence of tropomyosin crystals. The good agreement between the calculated birefringence values and the measured ones demonstrates the applicability of this theory. On the other hand, the remaining discrepancies of 15% between calculated and measured values indicate the limits of the theory. Other theories for the optical properties of macromolecules in solutions were developed by Cassim and Taylor (1965) and by Fortelny (1974) for the explanation of flow birefringence measurements. The new theories treat a solute molecule as a necklace of induced dipoles which are embedded in a solvent made from dipoles of different polarizability. The polarization of the solution in an external field is calculated by summing the interactions between nearby dipoles. This procedure allows to consider more realistically the local structure of the solution. It seems possible to apply this method to protein crystals for which the structure is known in great detail. If the optical properties of protein crystals were to be calculated with those refined methods, we expect an even better agreement between experiment and theory.

We use our model calculation to derive the intrinsic birefringence value of $\Delta n_2 = 0.011$ for the tropomyosin molecule. This value is close to the intrinsic birefringence of the helical polypeptide PBLG ($\Delta n_{PBLG} = 0.001$.) Δn_{PBLG} was measured by Cassim and Taylor (1965) with the PBLG molecules dissolved in a solvent that matches the average refractive index of the macromolecules. The same method can possibly be used to measure the intrinsic birefringence of the tropomyosin molecule more accurately. If the water in the crystal is exchanged by a solvent that matches the average refractive index of the protein, then the remaining optical anisotropy of the crytal is only a consequence of the intrinsic birefringence of the protein material. So far, an attempt by us to exchange the crystal water by a different solvent resulted in the decomposition

of the crystals. By fixing the crystals with glutaraldehyde a procedure might be found to stabilize the crystal structure and to make it suitable for a solvent exchange (Caspar et al., 1969).

Temperature Dependence

The two measured birefringence values Δn_a and Δn_b decreased with increasing temperature. The observation, that the measured value Δn_c did not change with temperature, seems to rule-out the possibility that the temperature change of Δn_a and Δn_b is caused only by a change in the refractive indices of the solvent or the protein. A change of the refractive indices affects all three birefringence values $\Delta n_{a,b,c}$. However, we were able to account for the measured change, at least in part, by assuming a change in unit cell parameters which is observed in x-ray diffraction experiments with tropomyosin crystals. Another contribution to the decrease in birefringence might come from increased molecular motion and large displacement amplitudes of the tropomyosin molecules in the crystal at higher temperature. Displacement amplitudes as large as 9Å were observed in x-ray diffraction expriments (Boylan and Phillips, 1986) with increasing amplitudes at higher temperatures. Random molecular motion makes the average crystal structure less anisotropic and therefore reduces the optical anisotropy of the crystal. We are currently studying the molecular motion in tropomyosin crystals by inelastic light-scattering experiments.

APPENDIX

In the appendix we derive the tensor of the excess polarizability of the tropomyosin filaments in the crystal. To this end, we first consider a single filament and we express its polarizability tensor $\underline{\alpha}_2$ in a coordinate system with the z-axis parallel to the filament axis. The tensor has then the diagonal form shown below:

$$\underline{\underline{\alpha}}_2 = \begin{bmatrix} \alpha_{2\perp} & 0 & 0 \\ 0 & \alpha_{2\perp} & 0 \\ 0 & 0 & \alpha_{2\parallel} \end{bmatrix} \qquad (14)$$

The expressions for $\alpha_{2\parallel}$ and $\alpha_{2\perp}$ are given in Eqs. 7 a and b.

The crystal is made from four sets of filaments. Filaments belonging to one set are all parallel to one another and are oriented along one of the four body diagonals of the rectangular unit cell. For the following calculations we consider the contents of only one unit cell vicarious for the whole crystal. This reduces one set of filaments to just one tropomyosin molecule with the polarizability tensor given in Eq. 14 (polarizabilities are expressed per unit volume). The polarizability tensor of the crystal is obtained by adding the polarizability tensors of all four tropomyosin molecules in the unit cell. We first express each tensor in the coordinate system of the crystallographic axes. The
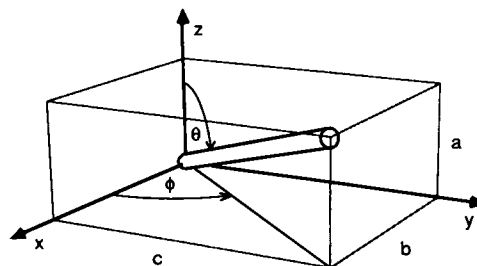

FIGURE 5 Illustration of the angles θ and ϕ by which one molecule is rotated to attain its position along the [111] direction in the unit cell.

transformation for each tensor is the matrix that rotates one molecule into its position along one of the four body diagonals of the unit cell. For example, the molecule parallel to the [111] direction attains its position from an original orientation parallel to the z-axis by a rotation in two steps illustrated in Fig. 5. The polarizability tensor of that molecule is given by:

$$\underline{\underline{\alpha}}_{[111]} = R^{-1}(\theta, \phi)\, \underline{\underline{\alpha}}_2 R(\theta, \phi) \qquad (15)$$

with:

$$R(\theta, \phi) = \begin{bmatrix} \cos\phi\,\cos\theta & \sin\phi\,\cos\theta & -\sin\theta \\ -\sin\phi & \cos\phi & 0 \\ \cos\phi\,\sin\theta & \sin\phi\,\sin\theta & \cos\theta \end{bmatrix}.$$

The same rotation matrix is used for the other three molecules in the unit cell, but the angles ϕ and θ are different for each molecule.

Finally we add the polarizabilities of all four molecules and express the trigonometric functions in terms of the unit cell parameters, and obtain the following terms for the diagonal polarizability tensor of the crystal:

$$\alpha_{11} = \{(\alpha_{2\parallel} - \alpha_{2\perp})(b^2/l^2) + \alpha_{2\perp}\}$$

$$\alpha_{22} = \{(\alpha_{2\parallel} - \alpha_{2\perp})(c^2/l^2) + \alpha_{2\perp}\}$$

$$\alpha_{33} = \{(\alpha_{2\parallel} - \alpha_{2\perp})(a^2/l^2) + \alpha_{2\perp}\}$$

with $l^2 = a^2 + b^2 + c^2$.

REFERENCES

Bailey, K. 1954. Structure proteins. II. muscle. *In* The Proteins. Vol II. H. Neurath, and K. Bailey, editors. Academic Press, Inc., New York.

Born, M., and E. Wolf. 1970. Principles of optics. Pergamon Press, Oxford.

Boylan, D., and G. N. Phillips. 1986. Motions of tropomyosin. Characterization of anisotropic motions and coupled displacements in crystals. *Biophys. J.* 49:76-78.

Bragg, W. L., and A. B. Pippard. 1953. The form birefringence of macromolecules. *Acta. Crystallogr.* 6:865-867.

Caspar, D. L. D., C. Cohen, and W. Longley. 1969. Tropomyosin: crystal structure, polymorphism, and molecular interactions. *J. Mol. Biol.* 41:87-107.

Cassim, J. Y., and E. W. Taylor. 1965. Intrinsic birefringence of poly-γ-benzyl-L-glutamate, a helical polypeptide, and the theory of birefringence. *Biophys. J.* 5:531-552.

Cervelle, B., F. Cesbron, J. Berthou, and P. Jollés. 1974. Morphologie et propriétés optiques des cristaux de lysozyme de poule de type quadratique et orthorhombique. *Acta. Crystallogr.* A30:645-648.

Fortelny, I. 1974. Solvent effects in flow birefringence of polymer solutions. General theory and discussion of form effects. *J. Polym. Sci. Polym. Phys. Ed.* 12:2319-2330.

Hartshorne, N. H., and A. Stuart. 1970. Crystals and the polarizing microscope. Fourth edition. Edward Arnold Publishers Ltd, London.

Holtzer, A., R. Clark, and S. Lowey. 1965. The conformation of native and denaturated tropomyosin B. *Biochem. Stry.* 4:2401-2411.

Kay, C. M. 1960. The partial specific volume of muscle proteins. *Biochim. Biophys. Acta.* 38:420-427.

Lodge, T. P., and J. L. Schrag. 1984. Oscillatory flow birefringence properties of polymer solutions at high effective frequencies. *Macromol.* 17:352-360.

Maret, G., M. v. Schickfus, A. Mayer, and K. Dransfeld. 1975. Orientation of nucleic acids in high magnetic fields. *Phys. Rev. Lett.* 35:397-400.

Maret, G., and K. Dransfeld. 1985. Biomolecules and polymers in high steady magnetic fields. *In* Topics in Applied Physics, Strong and ultrastrong magnetic fields. F. Herlach, editor. Springer-Verlag, Berlin, Heidelberg, New York. Vol. 57. 143-204.

O'Konski, C. T., and A. J. Haltner. 1957. Electric properties of macromolecules. I. A study of electric polarization in polyelectrolytic solutions by means of electric birefringence. *J. Am. Chem. Soc.* 79:5634-5649.

O'Konski, C. T., K. Yoshioka, and W. H. Orttung. 1959. Electric properties of macromolecules. IV. Determination of electric and optical parameters from saturation of electric birefringence in solutions. *J. Phys. Chem.* 63:1558-1565.

Perlmann, G. E., L. G. Longworth. 1948. The specific refractive increment of some purified proteins. *J. Am. Chem. Soc.* 70:2719-2721.

Perutz, M. F. 1953. Polarization dichroism, form birefringence, and molecular orientation in crystalline haemoglobins. *Acta. Crystallogr.* 6:859-864.

Peterlin, A., und H. A. Stuart. 1939. Zur Theorie der Strömungsdoppelbrechung von Kolloiden und großen Molekülen in Lösung. *Z. Physik.* 12:1-19.

Phillips, G. N., J. P. Fillers, and C. Cohen. 1986. Tropomyosin crystal structure and muscle regulation. *J. Mol. Biol.* 192:111-131.

Wiener, O. 1912. Die Theorie des Mischkörpers für das Feld der stationären Strömung. Erste Abhandlung. Die Mittelwertsätze für Kraft, Polarisation und Energie. *Abhandl. Math. Phys. Klas. Köngl. Sächs. Gesellsch. Wissensch.* 23:509-604.

Woods, E. F. 1967. Molecular weight and subunit structure of tropomyosin B. *J. Biol. Chem.* 242:2859-2871.